

Unsteady flow and heat transfer of viscous incompressible fluid with temperature-dependent viscosity due to a rotating disc in a porous medium

This article has been downloaded from IOPscience. Please scroll down to see the full text article.

2006 J. Phys. A: Math. Gen. 39 979

(<http://iopscience.iop.org/0305-4470/39/4/017>)

View [the table of contents for this issue](#), or go to the [journal homepage](#) for more

Download details:

IP Address: 171.66.16.106

The article was downloaded on 03/06/2010 at 04:51

Please note that [terms and conditions apply](#).

Retraction

Unsteady flow and heat transfer of viscous incompressible fluid with temperature-dependent viscosity due to a rotating disc in a porous medium

H A Attia 2006 *J. Phys. A: Math. Gen.* **39** 979–991

It has come to the attention of the Institute of Physics that this article should not have been submitted for publication owing to its plagiarism of an earlier paper (Hossain A, Hossain M A and Wilson M 2001 Unsteady flow of viscous incompressible fluid with temperature-dependent viscosity due to a rotating disc in presence of transverse magnetic field and heat transfer *Int. J. Therm. Sci.* **40** 11–20). Therefore this article has been retracted by the Institute of Physics and by the author, Hazem Ali Attia.

Unsteady flow and heat transfer of viscous incompressible fluid with temperature-dependent viscosity due to a rotating disc in a porous medium

Hazem Ali Attia¹

Department of Mathematics, College of Science, Al-Qasseem University, PO 237, Buraidah 81999, Saudi Arabia

Received 9 June 2005, in final form 2 October 2005

Published 11 January 2006

Online at stacks.iop.org/JPhysA/39/979

Abstract

This paper studies the effect of a porous medium and temperature-dependent viscosity on the unsteady flow and heat transfer for a viscous laminar incompressible fluid due to an impulsively started rotating infinite disc. The unsteady axi-symmetric boundary layer equations are solved using three methods, namely, (i) perturbation solution for small time, (ii) asymptotic analysis for large time and (iii) the finite difference method together with the Keller box elimination technique for intermediate times. The solutions are obtained in terms of local radial skin friction, local tangential skin friction and local rate of heat transfer at the surface of the disc, for different values of the pertinent parameters: the Prandtl number Pr , the viscosity variation parameter ε and porosity parameter m . The computed dimensionless velocity and temperature profiles for $Pr = 0.72$ are shown graphically for different values of ε and m .

PACS numbers: 47.11.+j, 47.60.+i, 47.15.-x, 47.65.+a

Nomenclature

r	radial coordinate
z	normal coordinate
u	radial velocity component
v	tangential velocity component
w	axial velocity component
C_p	specific heat at constant pressure
K	Darcy permeability
f	dimensionless radial velocity function

¹ On leave from: Department of Engineering Mathematics and Physics, Faculty of Engineering, El-Fayoum University, El-Fayoum, Egypt.

g	dimensionless tangential velocity function
h	dimensionless axial velocity function
t	time
T	temperature in the flow region
T_w	surface temperature
T_∞	temperature of the ambient fluid
m	porosity parameter
α	thermal diffusivity
ε	viscosity variation constant
\bar{q}	rate of heat transfer
q	dimensionless rate of heat transfer
Pr	Prandtl number
ρ_∞	density of the fluid
θ	temperature of the fluid
μ	temperature-dependent viscosity
μ_∞	viscosity in the ambient fluid
κ	thermal conductivity of the fluid
η	dimensionless normal distance
ν	kinematic coefficient of viscosity
Ω	angular velocity
τ	dimensionless time
$\bar{\tau}_r$	radial skin friction
$\bar{\tau}_\varphi$	tangential skin friction
τ_r	dimensionless radial skin friction
τ_φ	dimensionless tangential skin friction

1. Introduction

Rotating disc flow and heat transfer is one of the classical problems of fluid mechanics that has both theoretical and practical values. Heat transfer from a rotating body is of importance for the rotating components of various types of machinery, for example, computer disk drives [1] and gas turbine rotors [2]. In some applications where the rotating object is a candidate for overheating, and limitations exist on the allowable rotational speed, further heat removal is feasible by means of impingement. This is also a common cooling technique for some transmission gearings where the mechanism bearings are subject to impingement cooling by a liquid lubricant. The interaction of rotation and impingement creates a complex but powerful flow capable of increasing heat transfer considerably.

The rotating disc problem was first formulated by von Karman [3]. He showed that the Navier–Stokes equations for steady flow of a viscous incompressible fluid due to an infinite rotating disc can be reduced to a set of ordinary differential equations and solved them by an approximate integral method. Later, Cochran [4] obtained more accurate results by patching two series expansions. It is found that the disc acts like a centrifugal fan, the fluid near the disc being thrown radially outwards. This in turn impulses an axial flow towards the disc to maintain continuity.

Benton [5] improved Cochran's solutions and extended the hydrodynamics problem to flow starting impulsively from rest. Bodewadt [6] studied the inverse problem of the disc at rest and fluid at infinity rotating with uniform angular velocity. Roger and Lance [7] studied numerically a similar problem with the disc rotating with different angular velocity to that of

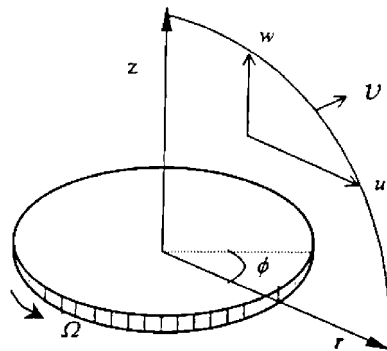


Figure 1. The flow configuration and coordinate system.

the surrounding fluid. Stuart [8], following a suggestion made by Batchelor [9] investigated the effect of uniform suction of fluid from the surface of the rotating disc. The effect of suction is essentially one of decreasing both radial and azimuthal components of the velocity and increasing the axial flow towards the disc at infinity. The boundary layer thinned, as a consequence. Ockendon [10] used the asymptotic method to determine the solutions of the problem for small values of suction parameter in the case of a rotating disc in a rotating fluid. Wagner [11], and Millsaps and Pohlhausen [12] determined the heat transfer from a disc with uniform surface temperature different from that of isothermal surroundings. Later, Sparrow and Gregg [13] obtained the heat transfer from a rotating disc to a fluid for arbitrary Prandtl number. Ostrach and Thornton [14], considering the same isothermal rotating disc, extended their investigation to a fluid with Prandtl number of 0.72 and variable physical properties. Hartnett [15] examined the influence of variation of surface temperature on the heat transfer from a disc rotating in still air, allowing the temperature difference between the disc surface and the fluid at rest to vary as a power function of radius.

In all the above studies, the viscosity of the fluid was assumed to be constant. However, it is known that this physical property may change significantly with temperature, and to predict the flow behaviour accurately it may be necessary to take into account viscosity variation for incompressible fluids. Graessley *et al* [16], and Mehta and Sood [17] showed that, when this effect is included, flow characteristics may be changed substantially compared to the constant viscosity assumption. The present investigation is concerned with the effect of temperature-dependent viscosity on the flow and heat transfer along a uniformly heated impulsively rotating disc in a porous medium. The flow in the porous medium deals with the analysis in which the differential equations governing the macroscopic fluid motion is based on the Darcy's law which accounts for the drag exerted by the porous medium [18–20].

2. Mathematical formalism

Let the disc lie in the plane $z = 0$ and the space $z \geq 0$ be occupied by homogeneous incompressible fluid in a porous medium, where z is the vertical axis in the cylindrical coordinate system with r and ϕ as the radial and tangential axes, respectively. The geometry of the problem is shown in figure 1. The disc rotates with uniform angular velocity Ω , T_w is the uniform temperature at the disc surface and T_∞ is the temperature of the ambient fluid. The flow is through a porous medium where the Darcy model is assumed [18–20]. The basic equations governing the flow of the fluid in the presence of the porous medium are as follows:

$$\frac{\partial u}{\partial r} + \frac{u}{r} + \frac{\partial w}{\partial z} = 0 \quad (1)$$

$$\rho_{\infty} \left(\frac{\partial u}{\partial t} + u \frac{\partial u}{\partial r} + w \frac{\partial u}{\partial z} - \frac{v^2}{r} + \frac{v}{K} u \right) = -\frac{\partial p}{\partial r} + \frac{\partial}{\partial r} \left(\mu \frac{\partial u}{\partial r} \right) + \frac{\partial}{\partial r} \left(\mu \frac{u}{r} \right) + \frac{\partial}{\partial z} \left(\mu \frac{\partial u}{\partial z} \right) \quad (2)$$

$$\rho_{\infty} \left(\frac{\partial v}{\partial t} + u \frac{\partial v}{\partial r} + \frac{uv}{r} + w \frac{\partial v}{\partial z} + \frac{v}{K} v \right) = \frac{\partial}{\partial r} \left(\mu \frac{\partial v}{\partial r} \right) + \frac{\partial}{\partial r} \left(\mu \frac{v}{r} \right) + \frac{\partial}{\partial z} \left(\mu \frac{\partial v}{\partial z} \right) \quad (3)$$

$$\rho_{\infty} C_p \left(\frac{\partial T}{\partial t} + u \frac{\partial T}{\partial r} + w \frac{\partial T}{\partial z} \right) = \kappa \left(\frac{\partial^2 T}{\partial r^2} + \frac{1}{r} \frac{\partial T}{\partial r} + \frac{\partial^2 T}{\partial z^2} \right). \quad (4)$$

The last term in the right-hand side of equations (2) and (3), named as Brinkman equations [21, 22], represents the Darcy force exerted by the fibres of the porous medium [18–20]. It should be pointed out that the characteristic length of the porous layer $K^{1/2}$ is taken as $K^{1/2} < 1$ for the Brinkman limit to be achieved [21, 22]. The boundary conditions for the present problem are

$$\begin{aligned} z = 0 : \quad & u, w = 0, \quad v = r\Omega, \quad T = T_w, \\ z \rightarrow \infty : \quad & u, v \rightarrow 0, \quad T \rightarrow T_{\infty}. \end{aligned} \quad (5)$$

To obtain the solutions of the governing equations, these are first converted into a convenient form using appropriate transformations. Considering this, we can introduce the following transformations:

$$\begin{aligned} u &= r\Omega \left(\frac{\tau}{1+\tau} \right) f(\eta, \tau), \quad v = r\Omega g(\eta, \tau), \quad w = -4\sqrt{\nu\Omega} \left(\frac{\tau}{1+\tau} \right)^{3/2} h(\eta, \tau), \\ \theta(\eta, \tau) &= \frac{T - T_{\infty}}{T_w - T_{\infty}}, \quad \eta = \frac{1}{2} \sqrt{\frac{\Omega}{\nu}} \left(\frac{\tau}{1+\tau} \right)^{1/2} z, \quad \tau = \Omega t. \end{aligned} \quad (6)$$

Now substituting the above transformations in equations (1)–(4), the following non-similarity equations are obtained:

$$\begin{aligned} (1 + \varepsilon\theta)h''' - \varepsilon\theta'h'' - (1 + \varepsilon\theta)^2 \left\{ 4 \left(\frac{1}{1+\tau} \right)^2 h' - 2\eta \left(\frac{1}{1+\tau} \right)^2 h'' + 4 \left(\frac{\tau}{1+\tau} \right) \frac{\partial h'}{\partial \tau} \right. \\ \left. + 4 \left(\frac{\tau}{1+\tau} \right)^2 g^2 - 8 \left(\frac{\tau}{1+\tau} \right)^2 hh'' - 4g^2 + 4 \left(\frac{\tau}{1+\tau} \right) mh' \right\} = 0 \end{aligned} \quad (7)$$

$$\begin{aligned} (1 + \varepsilon\theta)g'' - \varepsilon\theta'g' - (1 + \varepsilon\theta)^2 \left\{ 4 \left(\frac{\tau}{1+\tau} \right) \frac{\partial g}{\partial \tau} - 2\eta \left(\frac{1}{1+\tau} \right)^2 g' + 8 \left(\frac{\tau}{1+\tau} \right)^2 h'g \right. \\ \left. - 3 \left(\frac{\tau}{1+\tau} \right)^2 hg' + 4 \left(\frac{\tau}{1+\tau} \right) mg \right\} = 0 \end{aligned} \quad (8)$$

$$\frac{1}{Pr}\theta'' + 2\eta \left(\frac{1}{1+\tau} \right)^2 \theta' + 8 \left(\frac{\tau}{1+\tau} \right)^2 \theta'h = 4 \left(\frac{\tau}{1+\tau} \right) \frac{\partial \theta}{\partial \tau}. \quad (9)$$

It should be pointed out that equations (7)–(9) are dimensionless and that their solutions only depend on Pr , ε and m . The above equations should satisfy the following boundary conditions:

$$\begin{aligned} h(0, \tau) = h'(0, \tau) = 0, \quad g(0, \tau) = 1, \quad \theta(0, \tau) = 1, \\ h'(\infty, \tau) = g(\infty, \tau) = \theta(\infty, \tau) = 0 \end{aligned} \quad (10)$$

where $Pr (= \mu_{\infty} C_p / \kappa)$ is the Prandtl number, ε is termed the viscosity variation parameter and $m (= \mu_{\infty} / \rho_{\infty} K \Omega)$ is the porosity parameter. Throughout, prime denotes the differentiation with respect to η .

Since the system of equations (7)–(9) are locally non-similar by nature, we may obtain the solution by both the local non-similarity method introduced by Sparrow and Minkowycz [23] and the implicit finite difference method together with the Keller box elimination technique [24]. Here, we propose to simulate equations (7)–(9) by the finite difference method, since it is found to be efficient and accurate as well documented and widely used by Cebeci and Bradshaw [25]. According to the aforementioned method, the system of partial differential equations are first converted to a system of seven first-order differential equations by introducing new functions of the η derivatives. This system is then put into a finite difference scheme in which the resulting nonlinear difference equations are linearized by the use of Newton's quasi-linearization method. The resulting linear difference equations, along with the boundary conditions, are finally solved by an efficient block-tri-diagonal factorization method introduced by Keller [24].

The action of the viscosity in the fluid adjacent to the disc sets up a tangential shear stress, which opposes the rotation of the disc. As a consequence, it is necessary to provide a torque at the shaft to maintain a steady rotation. To find the tangential shear stress, $\bar{\tau}_\varphi$, we apply the Newtonian formula:

$$\bar{\tau}_\varphi = \left[\mu \left(\frac{\partial v}{\partial z} + \frac{1}{r} \frac{\partial w}{\partial \varphi} \right) \right]_{z=0}. \quad (11)$$

There is also a surface shear stress $\bar{\tau}_r$ in the radial direction, which can be obtained by applying the Newtonian formula:

$$\bar{\tau}_r = \left[\mu \left(\frac{\partial u}{\partial z} + \frac{1}{r} \frac{\partial w}{\partial r} \right) \right]_{z=0}. \quad (12)$$

The rate of heat transfer from the disc surface to the fluid is computed by the application of Fourier's law as

$$\bar{q} = -k \left(\frac{\partial T}{\partial z} \right)_{z=0}. \quad (13)$$

When the values of the functions h , g and θ are known, using the transformations given in (6), we can calculate the values of dimensionless radial skin friction, tangential skin friction and heat transfer rate from the following relation:

$$\begin{aligned} \tau_r(1+\varepsilon) &= \left(\frac{\tau}{1+\tau} \right)^{1/2} h''(0, \tau) \\ \tau_\varphi(1+\varepsilon) &= \left(\frac{\tau}{1+\tau} \right)^{-1/2} g'(0, \tau) \\ q &= - \left(\frac{\tau}{1+\tau} \right)^{-1/2} \theta'(0, \tau). \end{aligned} \quad (14)$$

3. Small time solution

For small time, i.e. when $\tau \ll 1$, then the transformations given in (6) take the following form:

$$\begin{aligned} u &= r\Omega\tau f(\eta, \tau), & v &= r\Omega g(\eta, \tau), & w &= -4\sqrt{\nu\Omega}\tau^{3/2}h(\eta, \tau), \\ \theta(\eta, \tau) &= \frac{T - T_\infty}{T_w - T_\infty}, & \eta &= \frac{1}{2}\sqrt{\frac{\Omega}{\nu\tau}}z, & \tau &= \Omega t. \end{aligned} \quad (15)$$

Introducing the above transformations, the flow governing equations (1)–(4) are reduced to the following non-similarity equations that are valid for small time:

$$(1 + \varepsilon\theta)h''' - \varepsilon\theta'h'' = (1 + \varepsilon\theta)^2 \left\{ 4h' - 2\eta h'' + 4\tau^2 h'^2 - 8\tau^2 h h'' - 4g^2 + 4m\tau h' + 4\tau \frac{\partial h'}{\partial \tau} \right\} \quad (16)$$

$$(1 + \varepsilon\theta)g'' - \varepsilon\theta'g' = (1 + \varepsilon\theta)^2 \left\{ 8\tau^2 h'g - 2\eta g' - 8\tau^2 h g' + 4m\tau g + 4\tau \frac{\partial g}{\partial \tau} \right\} \quad (17)$$

$$\frac{1}{Pr}\theta'' + 2\eta\theta' + 8\tau^2\theta'h = 4\tau \frac{\partial \theta}{\partial \tau}. \quad (18)$$

The boundary conditions are as follows:

$$\begin{aligned} h(0, \tau) = h'(0, \tau) = 0, \quad g(0, \tau) = 1, \quad \theta(0, \tau) = 1, \\ h'(\infty, \tau) = g(\infty, \tau) = \theta(\infty, \tau) = 0. \end{aligned} \quad (19)$$

It may be noted that equations (16)–(18) are non-similar partial differential equations by nature and of the parabolic type. Since $\tau \ll 1$, we can approximate the perturbation solutions of equations (16)–(18) by treating τ as the perturbation parameter. Hence, the functions h , g and θ can be assumed to be of the following form:

$$h(\eta, \tau) = \sum_{i=0}^{\infty} \tau^i h_i(\eta), \quad g(\eta, \tau) = \sum_{i=0}^{\infty} \tau^i g_i(\eta) \quad \text{and} \quad \theta(\eta, \tau) = \sum_{i=0}^{\infty} \tau^i \theta_i(\eta) \quad (20)$$

where $h_i(\eta)$, $g_i(\eta)$ and $\theta_i(\eta)$ are the functions depending on η . Now substituting expression (20) into equations (16)–(18) and taking the terms only up to $O(\tau^2)$ gives different problems that can be solved for the functions h_n , g_n and θ_n for $n = 0, 1, 2, \dots$ and are presented in the appendix.

Once the values of the functions h_n , g_n and θ_n for $n = 0, 1, 2, \dots$ and their derivatives are known, the values of dimensionless radial skin friction τ_r , tangential skin friction τ_ϕ and heat transfer rate q can easily be obtained from the following expressions:

$$\tau_r(1 + \varepsilon) = \tau^{1/2}h''(0, \tau), \quad \tau_\phi(1 + \varepsilon) = \tau^{1/2}g'(0, \tau), \quad q = -\tau^{-1/2}\theta'(0, \tau). \quad (21)$$

4. Large time solution

When $\tau \gg 1$ then the transformations given in (6) reduce to the following form:

$$\begin{aligned} r = r_0 f(\eta, \tau), \quad v = r\Omega g(\eta, \tau), \quad w = -4\sqrt{v\Omega}h(\eta, \tau), \\ \theta(\eta, \tau) = \frac{T - T_\infty}{T_w - T_\infty}, \quad \eta = \frac{1}{2}\sqrt{\frac{\Omega}{v}}z, \quad \tau = \Omega t. \end{aligned} \quad (22)$$

Using the above transformations, the flow governing equations (1)–(4) take the following form:

$$(1 + \varepsilon\theta)h''' - \varepsilon\theta'h'' - (1 + \varepsilon\theta)^2 \left\{ 4h'^2 - 4g^2 - 8hh'' + 4\frac{\partial h'}{\partial \tau} + 4mh' \right\} = 0 \quad (23)$$

$$(1 + \varepsilon\theta)g'' - \varepsilon\theta'g' - (1 + \varepsilon\theta)^2 \left\{ 8h'g - 8gh' + 4\frac{\partial g}{\partial \tau} + 4mg \right\} = 0 \quad (24)$$

$$\frac{1}{Pr}\theta'' + 8\theta'h = 4\frac{\partial \theta}{\partial \tau}. \quad (25)$$

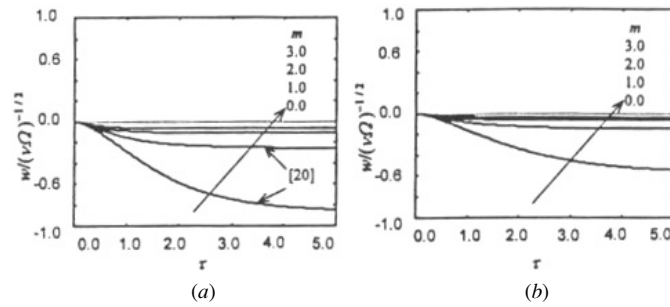


Figure 2. Time development of the axial velocity for (a) $\varepsilon = 0.0$ and (b) $\varepsilon = 2.0$ at infinity with different values of the porosity parameter m .

The boundary conditions to be satisfied by the above equations are

$$\begin{aligned} h(0, \tau) = h'(0, \tau) = 0, \quad g(0, \tau) = 1, \quad \theta(0, \tau) = 1, \\ h'(\infty, \tau) = g(\infty, \tau) = \theta(\infty, \tau) = 0. \end{aligned} \quad (26)$$

At the steady-state situation the τ -derivative in equations (23)–(25) can be neglected. Hence,

$$(1 + \varepsilon\theta)h''' - \varepsilon\theta'h'' - (1 + \varepsilon\theta)^2\{4h'^2 - 4g'^2 - 8h'g' + 4mh''\} = 0 \quad (27)$$

$$(1 + \varepsilon\theta)g'' - \varepsilon\theta'g' - (1 + \varepsilon\theta)^2\{8h'g - 8\theta'h + 4mg\} = 0 \quad (28)$$

$$\frac{1}{Pr}\theta'' + 8\theta'h = 0 \quad (29)$$

and the boundary conditions become

$$\begin{aligned} h(0) = h'(0) = 0, \quad g(0) = 1, \quad \theta(0) = 1, \\ h'(\infty) = g(\infty) = \theta(\infty) = 0. \end{aligned} \quad (30)$$

The solutions of the above sets of equations are obtained using the methods adopted in the preceding section. As before, once the values of the functions h , g and θ are known, we can calculate the values of dimensionless radial skin friction, tangential skin friction and heat transfer rate from the following relations:

$$\tau_r(1 + \varepsilon) = h''(0), \quad \tau_\phi(1 + \varepsilon) = g'(0), \quad q = -\theta'(0). \quad (31)$$

5. Results and discussion

Numerical simulations were carried out for the motion of a fluid having Prandtl number Pr equal to 0.72 (suitable for air), while the viscosity variation parameter $\varepsilon = 0.0, 1.0, 2.0$ and 3.0 . The results are presented in terms of non-dimensional local radial skin friction and tangential skin friction, as well as the rate of heat transfer at the disc surface, against the time-dependent parameter τ .

The growth of the axial velocity component against time is depicted in figure 2: (a) for $\varepsilon = 0.0$ and (b) for $\varepsilon = 2.0$, for different values of porosity parameter $m = 0.0, 1.0, 2.0$ and 3.0 and for $Pr = 0.72$. In figure 2(a), for constant viscosity ($\varepsilon = 0.0$), it can be seen that increasing the value of the porosity parameter m leads to a reduction in the (negative) axial velocity towards the disc, from -0.88 to -0.061 in the steady state. In figure 2(b), axial velocity reduces from -0.59 to -0.036 with increase in m for $\varepsilon = 2.0$. For the uniform

Table 1. Numerical values of the local rate of heat transfer q obtained by different methods for $Pr = 0.72$, and $\varepsilon = 0.0$ and 2.0 , and the porosity parameter $m = 0.0$ and 1.0 .

τ	$\varepsilon = 0.0$		$\varepsilon = 2.0$	
	Series and asymptotic	Keller box	Series and asymptotic	Keller box
$m = 0.0$				
0.01	0.9591 ^s	0.959 18	0.959 10 ^s	0.959 18
0.10	3.034 43 ^s	3.041 44	3.034 28 ^s	3.041 28
0.20	2.148 81 ^s	2.153 48	2.148 40 ^s	2.152 99
0.30	1.758 78 ^s	1.762 28	1.758 02 ^s	1.761 31
0.40	1.528 34 ^s	1.531 06	1.527 16 ^s	1.529 49
0.50	1.372 95 ^s	1.375 07	1.371 32 ^s	1.372 77
0.60	1.259 99 ^s	1.261 56	1.257 84 ^s	1.258 43
0.70	1.173 81 ^s	1.174 82	1.171 10 ^s	1.170 77
0.80	1.105 86 ^s	1.106 27	1.102 55 ^s	1.101 20
0.90	1.051 02 ^s	1.050 73	1.047 06 ^s	1.046 77
1.00	1.005 99 ^s	1.004 89	1.001 36 ^s	0.997 57
∞	0.657 19 ^a	0.657 19	0.575 43 ^a	0.575 43
$m = 1.0$				
0.0001	95.910 19 ^s	95.9186	95.910 19 ^s	95.9186
0.10	3.034 43 ^s	3.041 38	3.034 28 ^s	3.041 28
0.20	2.148 81 ^s	2.153 12	2.148 40 ^s	2.152 64
0.30	1.758 78 ^s	1.761 31	1.758 02 ^s	1.760 39
0.40	1.528 34 ^s	1.529 14	1.527 16 ^s	1.527 69
0.50	1.372 95 ^s	1.371 84	1.371 32 ^s	1.369 78
0.60	1.259 99 ^s	1.256 65	1.257 84 ^s	1.253 93
0.70	1.173 81 ^s	1.167 88	1.171 10 ^s	1.164 47
0.80	1.105 86 ^s	1.096 96	1.102 55 ^s	1.092 81
0.90	1.051 02 ^s	1.040 73	1.047 06 ^s	1.033 84
1.00	1.005 99 ^s	0.999 90	1.001 36 ^s	0.984 26
∞	0.335 80 ^a	0.335 80	0.273 30 ^a	0.273 30

^a For large r and ^s for small τ .

viscosity case, the porosity has more apparent effect on the axial velocity than in the case of variable viscosity (i.e., $\varepsilon \neq 0.0$).

Numerical values of the local rate of heat transfer, for $\varepsilon = 0.0$ and $\varepsilon = 2.0$ and different values of m for the fluid with $Pr = 0.72$, are displayed in table 1. From table 1 it can be seen that the effect of porosity parameter m on the heat transfer rate in the small-time-dominated regime is negligible for both values of the viscosity variation parameter ε . At the large-time-dominated regime, the porosity affects the rate of heat transfer significantly for both uniform and variable viscosity. An increase in the viscosity variation parameter ε leads to a decrease in the values of local heat transfer rate for each value of m far from the disc surface.

The perturbation solutions for small τ , asymptotic solutions for large τ and the finite difference solutions for the entire τ regime are illustrated in figures 3 and 4 for comparison. Comparison between these solutions shows excellent agreement in the respective regimes, i.e. for small and large times.

The effects of porosity parameter $m = 0.0, 1.0, 2.0$ and 3.0 on the dimensionless radial skin friction, as well as tangential skin friction, for the fluid with $Pr = 0.72$, are depicted in figures 3(a), 4(a) and 3(b), 4(b) for $\varepsilon = 0.0$ and $\varepsilon = 2.0$, respectively. From figure 3, it can be seen that an increasing value of m causes a decrease in radial skin friction, whereas the radial

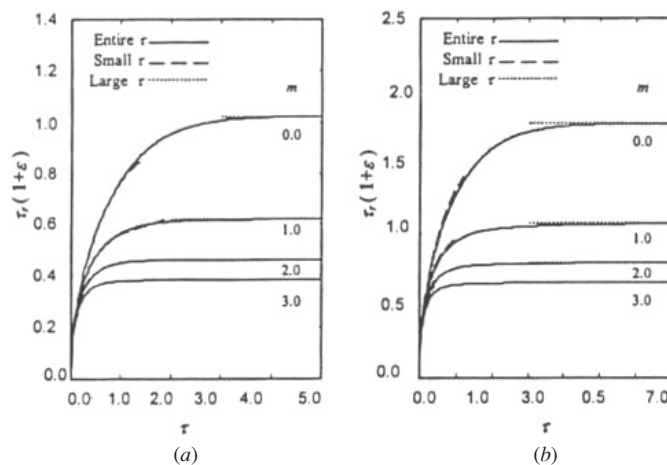


Figure 3. Non-dimensional radial skin friction $\tau_r(1+\varepsilon)$ against τ for different values of the porosity parameter m , while $Pr = 0.72$: (a) $\varepsilon = 0.0$ and (b) $\varepsilon = 2.0$.

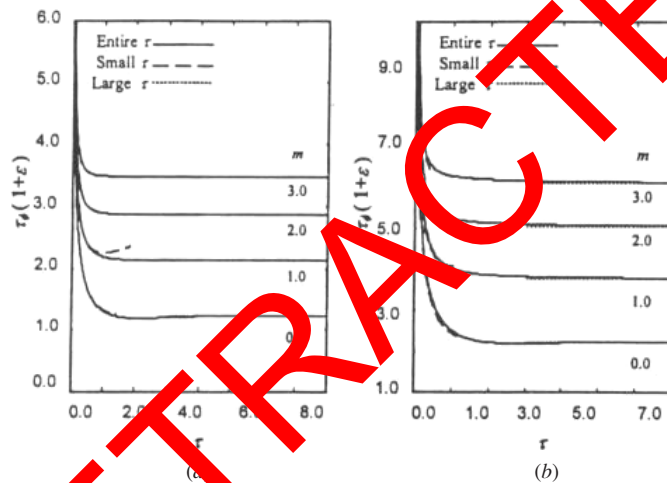


Figure 4. Non-dimensional tangential skin friction $\tau_\theta(1+\varepsilon)$ against τ for different values of the porosity parameter m , while $Pr = 0.72$: (a) $\varepsilon = 0.0$ and (b) $\varepsilon = 2.0$.

skin friction increases monotonically as τ increases and eventually reaches a constant value. Further inspection of figure 3 reveals the fact that the approach of the radial skin friction to the asymptotic state becomes slower as ε increases.

From figure 4, it is observed that the tangential skin friction decreases with a decrease in the values of the porosity parameter m . Further, it may be seen that the tangential skin friction decreases monotonically as τ increases up to a steady-state value. Increasing value of ε leads to a decrease in values of dimensionless radial velocity. Further inspection of figure 5(a) reveals that an increase in the porosity parameter m causes a significant decrease in radial velocities and thinning of the momentum boundary layer. In the non-porous case ($m = 0.0$) and for constant viscosity, the maximum radial velocity appears at $\eta = 0.45$; whereas for $m = 1.0$, the maximum radial velocity appears at $\eta = 0.30$, i.e. the point of maximum

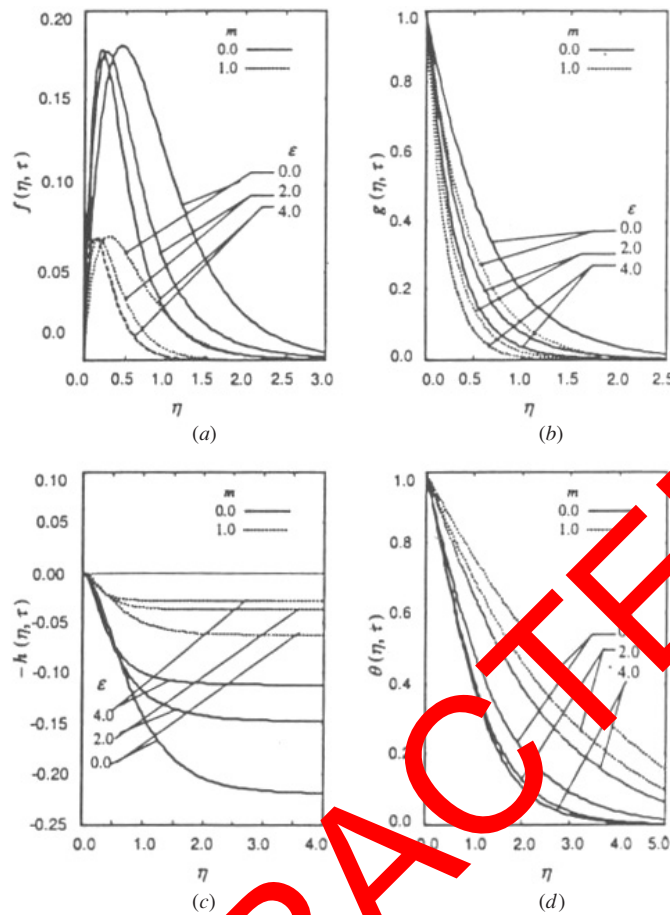


Figure 5. The dimensionless (a) friction $f(\eta, \tau)$, (b) tangential velocity profile $g(\eta, \tau)$, (c) axial velocity profile $-h(\eta, \tau)$ and (d) temperature profile $\theta(\eta, \tau)$ against η for different values of $\varepsilon = 0.0, 2.0, 4.0$ and with $m = 0.0, 1.0$ for $Pr = 0.72$.

radial velocity moves closer to the surface of the disc. In figure 5(b), we see that an increase in ε also leads to a decrease in tangential velocities in the boundary layer for both values of the porosity parameter ($m = 0.0$ and 1.0). In figure 5(c), the non-dimensional (negative) axial velocity decreases negatively from 0.22 to 0.11 with increase in the value of ε for $m = 0.0$. In the porous case ($m = 1.0$), the axial velocity more rapidly approaches the steady-state situation with increase in the viscosity variation ε . From figure 5(d), it may be observed that temperature profiles and the thermal boundary layer thickness increase with increasing value of ε for both $m = 0.0$ and $m = 1.0$.

6. Conclusions

In this paper, the effects of porosity of the medium and temperature-dependent viscosity on the behaviour of unsteady flow of an incompressible viscous fluid due to an impulsively started rotating disc have been investigated. The local non-similarity equations governing the unsteady flow and heat transfer are developed for small time and large time regimes as

well as in the entire time regime. Different solution methodologies have been employed for the complete integration of the resulting non-similarity equations, namely, (i) perturbation solutions, (ii) asymptotic solutions and (iii) implicit finite difference methods with the Keller box elimination technique, for small time and large time regimes as well as in the entire time regime, as appropriate.

From the present investigation, we can draw the following conclusions:

- (1) The solutions obtained for the cases of small time regime and large time regime are found to be in excellent agreement with that for the entire time regime, at every selected value of the porosity parameter m over the range of $0 \leq \tau \leq 8$ with $\varepsilon = 0.0$ and 2.0 , and $Pr = 0.72$.
- (2) At the surface of the disc, the local radial skin friction increases, whereas the local tangential skin friction decreases with increasing values of the time-dependent rotating parameter τ in both the porous and non-porous cases until the steady-state flow limit is reached.
- (3) Increasing the value of the viscosity variation parameter $\varepsilon = 0.0, 2.0$ and 4.0 leads to decrease in the values of radial and tangential velocity profile in both the porous and non-porous cases for the fixed value of Prandtl number $Pr = 0.72$.
- (4) Increasing the value of the viscosity variation parameter $\varepsilon = 0.0, 2.0$ and 4.0 reduces the axial velocity towards the disc surface for both cases $m = 0.0$ and $m = 1.0$.
- (5) The effect of increasing the value of the viscosity variation parameter $\varepsilon = 0.0, 2.0$ and 4.0 on the dimensionless radial, tangential and axial velocity profiles is to reduce the momentum boundary layer thickness, for both cases when $m = 0.0$ and 1.0 for Prandtl number $Pr = 0.72$.
- (6) As the value of the viscosity variation parameter ε increases, values of dimensionless temperature also increase for both cases $m = 0.0$ and $m = 1.0$. This effect causes a small increase in the thermal boundary layer thickness in the non-porous case, but for $m = 1.0$ there is a greater increase in the thermal boundary layer thickness for Prandtl number $Pr = 0.72$.
- (7) The effect of the porosity parameter $m = 0.0$ and 1.0 on the local rate of heat transfer is negligible near the disc surface for $\varepsilon = 0.0$ and 2.0 , but at the outer edge of the disc surface significant effects are found on the heat transfer rate for both values of m , again for $Pr = 0.72$.

Appendix

$$(1 + \varepsilon\theta_0)h_0''' - \varepsilon\theta_0'h_0'' - (1 + \varepsilon\theta_0)^2 \{4h_0' - 2\eta h_0'' - 4g_0^2\} \quad (\text{A.1})$$

$$(1 + \varepsilon\theta_0)g_0'' - \varepsilon\theta_0'g_0' - 2\eta(1 + \varepsilon\theta_0)^2 g_0' \quad (\text{A.2})$$

$$\frac{1}{Pr}\theta_0'' + 2\eta\theta_0' = 0 \quad (\text{A.3})$$

$$h_0(0) = h_0'(0) = 0, \quad g_0(0) = \theta_0(0) = 1, \quad h_0'(\infty) = 0, \quad g_0(\infty) = \theta_0(\infty) = 0 \quad (\text{A.4})$$

$$(1 + \varepsilon\theta_0)h_1''' + \varepsilon(\theta_1 h_0''' - \theta_1' h_0'' - \theta_0' h_1'') - (1 + \varepsilon\theta_0)^2 \{8h_1' - 2\eta h_1'' - 8g_0 g_1 + 4m h_0'\} \\ - (2\varepsilon\theta_1 + 2\varepsilon^2\theta_0\theta_1) \{4h_0' - 2\eta h_0'' - 4g_0^2\} = 0 \quad (\text{A.5})$$

$$(1 + \varepsilon\theta_0)g_1'' + \varepsilon(\theta_1 g_0'' - g_0' \theta_1' - g_1' \theta_0') - (1 + \varepsilon\theta_0)^2 \{4g_1 - 2\eta g_1' + 4m g_0\} \\ + 2\eta(2\varepsilon\theta_1 + 2\varepsilon^2\theta_0\theta_1) g_0' = 0 \quad (\text{A.6})$$

$$\frac{1}{Pr}\theta_1'' + 2\eta\theta_1' = 4\theta_1 \quad (\text{A.7})$$

$$\begin{aligned} h_1(0) = h_1'(0) = 0, \quad g_1(0) = \theta_1(0) = 0, \\ h_1'(\infty) = 0, \quad g_1(\infty) = \theta_1(\infty) = 0 \end{aligned} \quad (\text{A.8})$$

$$\begin{aligned} (1 + \varepsilon\theta_0)h_2''' + \varepsilon(\theta_2h_0''' + \theta_1h_1''' - \theta_2'h_0'' - \theta_1'h_1'' - \theta_0'h_2'') \\ - (1 + \varepsilon\theta_0)^2 \{12h_2' - 2\eta h_2'' + 4h_0'^2 - 8h_0'h_0'' - 8g_0g_2 - 4g_1^2 + 4mh_1'\} \\ - (2\varepsilon\theta_1 + 2\varepsilon^2\theta_0\theta_1) \{8h_1' - 2\eta h_1'' - 8g_0g_1 + 4mh_0'\} \\ - (2\varepsilon\theta_2 + \varepsilon^2(2\theta_0\theta_2 + \theta_1^2)) \{4h_0' - 2\eta h_0'' - 4g_0^2\} = 0 \end{aligned} \quad (\text{A.9})$$

$$\begin{aligned} (1 + \varepsilon\theta_0)g_2'' + \varepsilon(\theta_2g_0'' + \theta_1g_1'' - \theta_2'g_0' - \theta_1'g_1' - \theta_0'g_2') \\ - (1 + \varepsilon\theta_0)^2 \{8g_2 - 2\eta g_2' + 8h_0'g_0 - 8g_0'h_1 + 4mg_1\} \\ - (2\eta(2\varepsilon\theta_2 + \varepsilon^2(2\theta_0\theta_2 + \theta_1^2))g_0' = 0 \end{aligned} \quad (\text{A.10})$$

$$\frac{1}{Pr}\theta_2'' + 2\eta\theta_2' - 8\theta_0'h_0 = 8\theta_2 \quad (\text{A.11})$$

$$\begin{aligned} h_2(0) = h_2'(0) = 0, \quad g_2(0) = \theta_2(0) = 0, \\ h_2'(\infty) = 0, \quad g_2(\infty) = \theta_2(\infty) = 0 \end{aligned} \quad (\text{A.12})$$

It can be seen that equations (A.1) and (2) are coupled and nonlinear by nature for the case of a fluid possessing variable viscosity ($\varepsilon \neq 0.0$) and the solution of which is not possible analytically. A similar situation prevails for the subsequent sets. Numerical solutions of equations (A.1)–(A.4) are obtained using the Nachtsheim–Swigert iteration [26] together with the sixth-order implicit Runge–Kutta–Butcher [27] initial value solver. Solutions of the subsequent sets of equations (A.5)–(A.11) are also obtained by the above method for different values of the pertinent parameters.

References

- [1] Herrero J, Humphery J A C and Gault F 1994 Comparative analysis of coupled flow and heat transfer between co-rotating disks in rotating and fixed cylindrical enclosures *Am. Soc. Mech. Eng. Heat Transfer Div.* **300** 111–21
- [2] Owen J M and Rogers G H 1989 Flow and heat transfer in rotating disk systems *Rotor–Stator Systems* vol 1 (Taunton, New York: Research Studies Press/Wiley)
- [3] Von Kármán T 1921 Über laminare und turbulente Reibung *Z. Angew. Math. Mech.* **1** 233–55
- [4] Cooley W C 1934 The flow due to a rotating disk *Proc. Camb. Phil. Soc.* **30** 365–75
- [5] Benton F R 1966 On the flow due to a rotating disk *J. Fluid Mech.* **24** 781–800
- [6] Bodewadt L T 1940 Die Drehströmung über festem Grunde *Z. Angew. Math. Mech.* **20** 241–53
- [7] Rogers M C and Lance G N 1960 The rotationally symmetric flow of a viscous fluid in presence of infinite rotating disk *J. Fluid Mech.* **7** 617–31
- [8] Stuart J T 1954 On the effect of uniform suction on the steady flow due to a rotating disk *Q. J. Mech. Appl. Math.* **7** 446–57
- [9] Batchelor G K 1951 Note on a class of solutions of the Navier–Stokes equations representing steady non-rotationally symmetric flow *Q. J. Mech. Appl. Math.* **4** 29–41
- [10] Ockendon H 1972 An asymptotic solution for steady flow above an infinite rotating disk with suction *Q. J. Mech. Appl. Math.* **25** 291–301
- [11] Wagner C 1948 Heat transfer from a heated disk to ambient air *J. Appl. Phys.* **19** 837–41
- [12] Millsaps K and Pohlhausen K 1952 Heat transfer by a laminar flow from a rotating plate *J. Aerosol Sci.* **19** 120–6

- [13] Sparrow E M and Gregg J L 1959 Heat transfer from a rotating disk to a fluid at any Prandtl number *ASME J. Heat Transfer C* **81** 249–51
- [14] Ostrach S and Thornton P R 1958 Compressible laminar flow and heat transfer about a rotating isothermal disk *NACA Technical Note* 4320
- [15] Hartnett J P 1959 Heat transfer from a non-isothermal rotating disk in still air *ASME J. Appl. Mech.* **4** 672–3
- [16] Gary J, Kassory D R, Tadjeran H and Zebib A 1982 The effect of significant viscosity variation on convective heat transport in water-saturated porous media *J. Fluid Mech.* **117** 233–49
- [17] Mehta K N and Sood S 1992 Transient free convection flow with temperature dependent viscosity in fluid saturated porous medium *Int. J. Eng. Sci.* **30** 1083–7
- [18] Joseph D D, Nield D A and Papanicolaou G 1982 Nonlinear equation governing flow in a saturated porous media *Water Resources Res.* **18** 1049–52
- [19] Ingham D B and Pop I 2002 *Transport Phenomena in Porous Media* (Oxford: Pergamon)
- [20] Khaled A R A and Vafai K 2003 The role of porous media in modeling flow and heat transfer in biological tissues *Int. J. Heat Mass Transfer* **46** 4989–5003
- [21] Howells I D 1998 Drag on fixed beds of fibers in slow flow *J. Fluids Mech.* **335** 163–92
- [22] Feng J, Ganatos P and Weinbaum S 1998 Motions of a sphere near planar confining boundaries in a Brinkman medium *J. Fluid Mech.* **375** 261–92
- [23] Minkowycz W J and Sparrow 1978 Numerical solution scheme for local non-similarity boundary layer analysis *Numer. Heat Transfer* **1** 69–85
- [24] Keller H B 1978 Numerical methods in the boundary layer theory *Annu. Rev. Mech.* **33** 417–35
- [25] Cebeci T and Bradshaw P 1984 *Physical and Computational Aspects of Convective Heat Transfer* (New York: Springer)
- [26] Nachtsheim P R and Swigert P 1965 Satisfaction of the asymptotic boundary conditions in numerical solution of the system of non-linear equations of boundary layer type *NASA TN D-3004*
- [27] Butcher J C 1964 Implicit Runge–Kutta process *Math. Comput.* **18** 50–5